Research Article

Landslide Susceptibility Mapping Using Frequency Ratio and Weight of Evidence Models in Purchaudi Municipality, Baitadi District, Nepal

Prakash Bahadur Ayer[1], Bharat Prasad Bhandari[1,2]
[1]College of Applied Sciences, Tribhuvan University, Kathmandu, Nepal
[2]Central Department of Environmental Sciences, Tribhuvan University, Kirtipur, Nepal
Corresponding Author: bbhandari@cdes.edu.np

Abstract
Landslides are prevalent in the Himalayas, resulting in annual fatalities and economic losses during the monsoon season. Various studies are conducted for landslide susceptibility mapping in the Himalayas; however, many rural settlements are under the threat of landslide. The main objective of this study is to prepare the landslide susceptibility map by using the bivariate frequency ratio (FR) and weight of evidence (WoE) models. For this study, the landslide inventory map was initially developed, allocating 70% of the data for training and 30% for testing by using Landsat-8, Google Earth, and Sentinel imageries. After a thorough examination of existing literature and extensive field research, a total of twelve potential factors that can cause landslides were selected. The success and prediction rate of both models were obtained by using the area under the curve (AUC) method. The findings show that the landslide susceptibility maps prepared by the weight of evidence (WoE) and the frequency ratio (FR) models are more or less similar and have similar prediction and accuracy rates. Both the WoE and FR models exhibit a success rate of 0.703. Similarly, the accuracy rates of the FR and WoE models are 0.777 and 0.775, respectively. Both models have an accuracy and prediction rate that exceeds 70%, making them suitable for evaluating landslide susceptibility in the same terrains of Sudurpaschim province. However, the frequency ratio model shows slightly better predictive ability compared to WoE. The landslide densities derived from both models exhibit a gradual increase from low to very high susceptibility class. Nevertheless, there is no significant difference in the success and prediction rates between the two models. This result may be useful as a reference for future studies on similar terrain in Nepal.

Keywords: Frequency ratio, landslide susceptibility, Sudurpaschim, weight of evidence

Introduction

Landslide is the movement of a mass of earth, rock, or debris down a slope (Cruden & Varnes, 1996). In the Himalayas, landslides are thought to constitute one of the most frequent geological hazards. People and infrastructure are vulnerable to landslide hazards since many hillside areas in Nepal are situated either directly on or next to unstable slopes and paleo landslide zones that periodically suffer recurrent instability (Thapa, 2015). Understanding the geographical distribution of landslides is crucial to reducing the impact of these natural disasters on people and property since it may be used to identify places that are at risk of landslides owing to their propensity to occur (Dai et al., 2011; Collins et al., 2012; Petley, 2012). Landslide initiation and development is the dynamic process in the Nepal Himalaya where it takes a decade for landslide evolution (Bhandari & Dhakal, 2021).

According to Bhandari et al. (2024), landslides in Nepal caused losses of USD 1,311,267 in 2021, resulting in 92 deaths, 80 injuries, and damage to 1,968 houses. Creating precise and effective landslide susceptibility maps can greatly enhance disaster prevention and mitigation efforts, while also assuring adequate public safety. Consequently, landslides pose a significant threat to the human life and environmental integrity, despite the publication of numerous research on landslide modeling in Nepal over the past few decades.

A number of variables relating to geology, geomorphology, land use and cover, rainfall, seismicity, human activity, etc. should be assessed in order to reduce the damage caused by landslides (Guzzetti et al., 2012). With the ability to create complete databases, thematic data layers, and spatial analyses of causative elements utilizing field data and remote sensing information, Geographic Information System (GIS) has become a vital tool in landslide research (Pradhan, 2010). In the field of landslide hazard management, landslide inventories created from Google Earth images, GIS, and remotely sensed data of a particular study area have proven to be extremely valuable tools (Guzzetti et al., 2012). These resources are essential for assessing landslide susceptibility, hazard potential, and related risks (Aleotti & Chowdhury, 1999). In recent years, landslide susceptibility maps have been created for many regions across the globe using GIS. Several thematic layers have been integrated using a variety of techniques in Nepal Himalaya, such as frequency ratio (FR),weight of evidence (WoE), analytical hierarchy process (AHP), and logistic regression (LR) (Lee & Sambath, 2006; Khan et al., 2019; Jana et al., 2019; Thapa & Bhandari, 2019; Pokharel & Bhandari, 2019; Armas, 2012; Getachew & Meten, 2011; Bhandari et al., 2024; Ercanoglu et al., 2008; Pourghasemi et al., 2018; Kayastha et al., 2013; Hung et al., 2017; Rasyid et al., 2016; Sun et al., 2022). Out of all of them, the frequency ratio and weight of evidence models are the most popular for efficiently

determining a person's vulnerability to landslides (Regmi et al., 2014, Bhandari et al., 2024).

For a long time, the Sudurpaschim province of Nepal has been grappling with a number of landslide issues (Manchado et al., 2021). Several large to very large landslides in the Baitadi District of Nepal are posing a threat to the safety of people and developmental activities. There is a huge gap in the landslide investigation and susceptibility assessment in the Baitadi District. This study compares the weight of evidence (WoE) with the frequency ratio (FR) model for mapping landslide susceptibility in the Purchaudi Municipality of Baitadi District, Nepal. The landslide susceptibility map obtained from this work is useful for the study area to develop disaster risk management plans and procedural act. These findings may be helpful as a reference for further studies in the similar terrains of the Sudurpaschim province and other parts of the country.

Materials and methods
Study area
Purchaudi Municipality is situated in the Baitadi District of the Sudurpaschim Province of Nepal (Fig.1). It is positioned in a latitude range of 29.67º to 29.52º north and a longitude range of 80.58º to 80.79º east. Bajhang District is situated to the east of this Municipality, while Dogdakedar Rural Municipality lies to the west. Dilashaini Rural Municipality is located to the north, and

Surnaya and Sigash Rural Municipality are situated to the south. The majority of the region's topography consists of undulating terrain with precipitous inclines. The study area is situated at an elevation ranging from 911 to 2705 meters above sea level. As to the Hydrology and Meteorological Department of Nepal, the highest temperature recorded in the Baitadi District is 38 ºC, while the lowest temperature is 7.1ºC. The average annual rainfall in the district ranges from 1646.8 to 2191.79 millimeters. Ruini Gad, Baggad, and Loligad are the tributary streams that contribute to the Tribeni watershed. The tributaries of streams converge with the primary Mahakali River, located 5 km west of Purchaundi.

Methods of data collection
The initial step involved collecting spatial data and extracting relevant factors to achieve the primary objective of creating a landslide susceptibility map. These factors were then analyzed to determine their relationship with landslides, and the results were validated. Data collection involved collecting primary and secondary data for creating a spatial inventory map. The process included interpreting aerial photos, utilizing tools like Google Earth, and employing remote sensing data and GIS. Thematic data layers for different landslide factors were then prepared to aid in generating the final landslide susceptibility map.
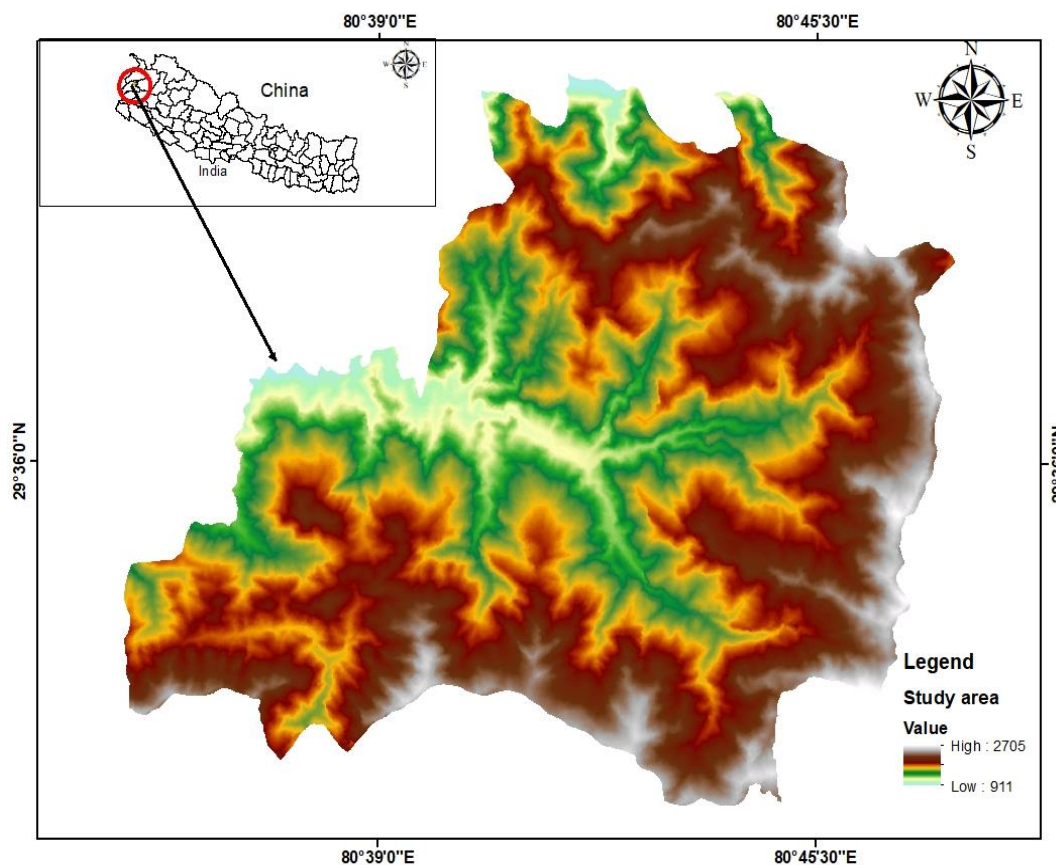

Figure 1. Location map of the study area

Primary data collection

The primary data collection involved field observations supported by instruments such as GPS and a checklist. During field visits, specific landslide sites were selected, and detailed photographs were captured to enhance understanding. Following the initial visit, a comprehensive inventory map of the landslides was generated. This map was created utilizing tools like Google Earth, Landsat and ArcGIS 10.8.2 version. Subsequently, a second round of field verification was executed, during which additional checklists were completed. As part of this second field visit, Key Informant Interview (KIIs) were also conducted to recognize old landslides. The new and recent landslides were observed and studied in the field. More than 70% landslides were verified in the field. Some of the recent landslides are shown in figures 2 a, b, c, & d.

Secondary data collection

The research area's overall assessment of landslide susceptibility utilized a combination of several methods and data sources. The evaluation procedure utilized ArcGIS 10.8.2, Google Earth, open street map, USGS data, meteorological data, and geological information. The field verification of landslide locations was crucial in ensuring accuracy and generating a detailed inventory map. This process was guided by data obtained from Google Earth. In order to create a map that identifies the factors that contribute to landslides, a Digital Elevation Model (DEM) with a resolution of 12.5 meters was obtained from the Alos Palsar. A thorough map was created by integrating many parameters such as slope, aspect, TWI, profile curvature, plane curvature, and SPI. ArcMap was employed open street map data to do Euclidean distance calculations, which helped in identifying regions near roads and rivers that are prone to landslides. The analysis of rainfall patterns was crucial. By using an Inverse Distance Weighting (IDW) interpolation approach to a dataset spanning a period of 12 years (2011-2023) collected from three stations (Chainpur west, Patan west, and Pipalkot), a rainfall map was constructed. This map provided insights into the distribution of rainfall and its possible consequences in triggering landslides. The geological map developed by Department of Mine and Geology was used to correlate landslide susceptibility with geological units. The statistical computations described in the document were performed, most likely including the analysis of a dataset to establish susceptibility to the Purchaundi municipality. This is an important step in assessing the total susceptibility to landslides.

Landslide conditioning factors

The event-controlling factors are known as "predisposing factors", "causative factors", "causal factors", "intrinsic factors", "conditioning factors", "quasi-static factors," and "preparatory factors" (Zhu et al., 2014). Identifying landslides and developing landslide susceptibility maps are critical steps in disaster preparation that can assist planners, local governments, and decision-makers (Kavzoglu et al., 2014). For this study, eleven landslide causative factors were selected based on literature and field observation. The factors having visual effects and prior possibility to trigger landslides are selected for preparing susceptibility maps.

Slope

The different types of slope movements observed result from various conditions that render the slope unstable, ultimately triggering movement (Karimi et al., 2011). Mass wasting or sliding events are more noticeable on steep terrain compared to gentle slopes. In the study area, a slope map was generated from a 12.5×12.5 m resolution DEM using the "Raster Surface" method. The slope angles in study area varied from 0° to 73° and which were classified into different zones, i.e., <17°, 17-27°, 27-35°, 35-46°, and >46°, as illustrated in Figure 3a.

Aspect

Aspect plays an important role in the occurrence of landslides. Since it can influence the moisture levels in the soil within a specific region. The orientation of the landscape affects several processes, including evapotranspiration, rainfall patterns, exposure to sunlight, and wind patterns. Besides this , the aspect of a slope impacts the amount of sunlight it receives and the conditions of seepage and groundwater (Hamza & Raghuvanshi, 2017). In a particular study investigation, a GIS tool was used to create an Aspect map from a DEM with a 12.5 m resolution. The aspect values within the study area span from -1 to 359.524 degrees, signifying the slope's directional orientation. These values were subsequently categorized into eight classes: north, northeast, east, southeast, south, southwest, west, and northwest, as illustrated in figure 3b.

Elevation

The elevation is not directly affected on landslide occurrence, but it impacts other factors such as rainfall, tectonic activities etc. Elevation factors affect landslide susceptibility because the higher the elevation, the higher the chances of a landslide. These factors were taken from DEM and categorized into five groups, as shown in figure 3c.

Topographic wetness index (TWI)

Different researchers have utilized topographic indices to elucidate how soil moisture is distributed across different geographical areas (Burt & Butcher 1986); (Moore et al., 1991). The TWI was developed (Beven & Kirkby, 1979) within the runoff model TOP MODEL. TWI is a commonly used approach that combines both the local upslope contributing area and the general slope of the terrain to quantify how topography affects hydrological processes. It is expressed as:

$$TWI = \ln (a / \tan \beta)$$

Where "a" represents the accumulated upslope area that drains through a specific point per unit contour length, "tan β" represents the slope angle at that point. In the study, TWI was regarded as an additional influencing factor, as illustrated in Fig. 3d.

Figure 2. a) Dandpur Mega Landslide b) Landslide occurred on the slopy terrace c) Landslide on the agriculture land near read section d) Landslide on the settlement area
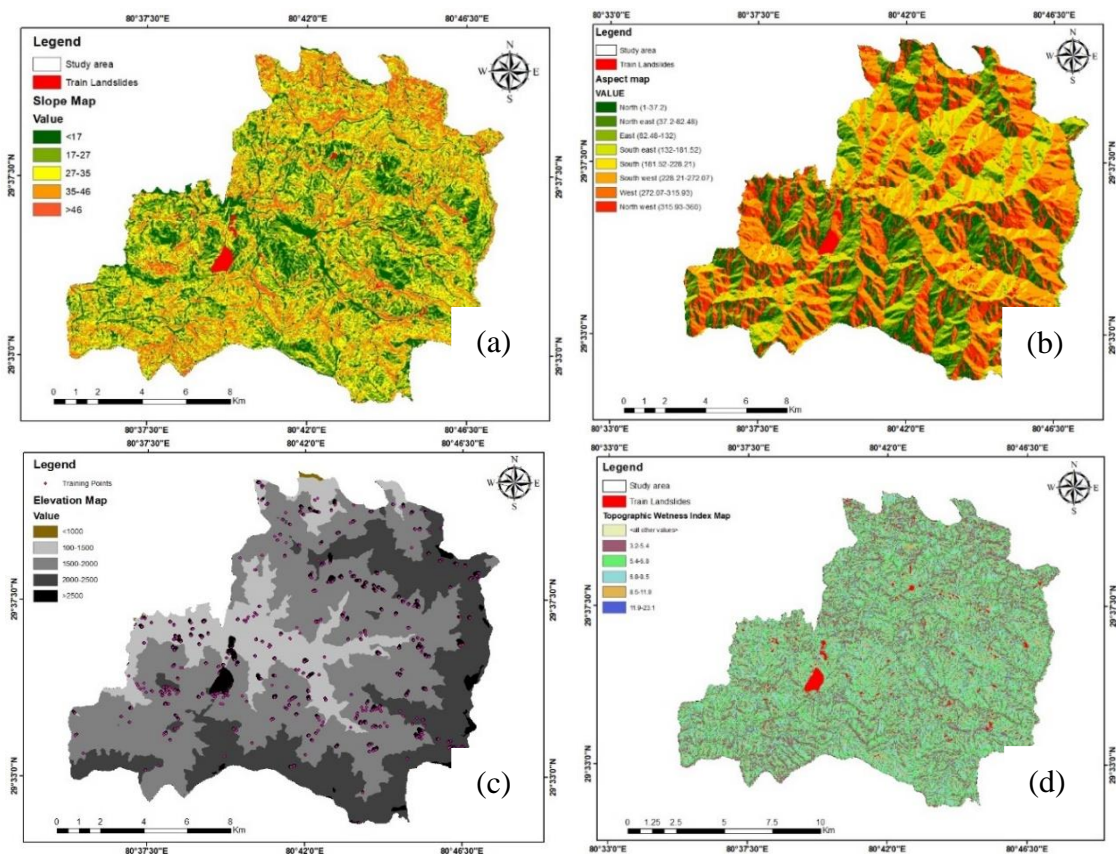

Figure 3. a) Slope map b) Aspect map c) Elevation map d) Topographical wetness index map of the study area

TU-CDES

Curvature

Curvature also plays a vital role in landslide occurrence. In Geo-science, curvature refers to the various curved features present in landscapes. Curvature is basically classified into three classes: concave, planar, and convex. In this study, a curvature map was generated from a DEM map with a resolution of 12.5×12.5 using ArcGIS software. These curvature values represent the topographic morphology of the area (Lee & Min, 2001). The profile curvature and plane curvature maps are shown in Figure 4a and Figure 4b.

Stream power index

The stream power index can be used to describe potential flow erosion at the given point of the topographic surface. As the catchment area and slope gradient increase, the amount of water contributed by upslope areas and the velocity of water flow increase; hence stream power index and landslide and erosion risk increase stream power index maps are shown in Fig. 4c.

The SPI map was created by using the following equation:

$$SPI = \ln(A * \tan(S))$$

Where 'A' represents the area of land that directs water flow towards a specific pixel, and 'S' represent the gradient of the local slope in degrees.

Distance to stream

In areas with soft lithology like mountainous terrain, rivers can trigger landslides by eroding the base of slopes and introducing water. To account for this in the study, river buffers were created. These buffers were generated by digitizing river locations from topographical maps and using the Euclidean distance tool. Within the study region, the categorical values for distance from the river ranged from 0 to 800 meters. These values were further divided into five classes: 0-100, 100-200, 200-300, 300-400, 400-500, and >500 meters, which is shown in Fig. 4d.
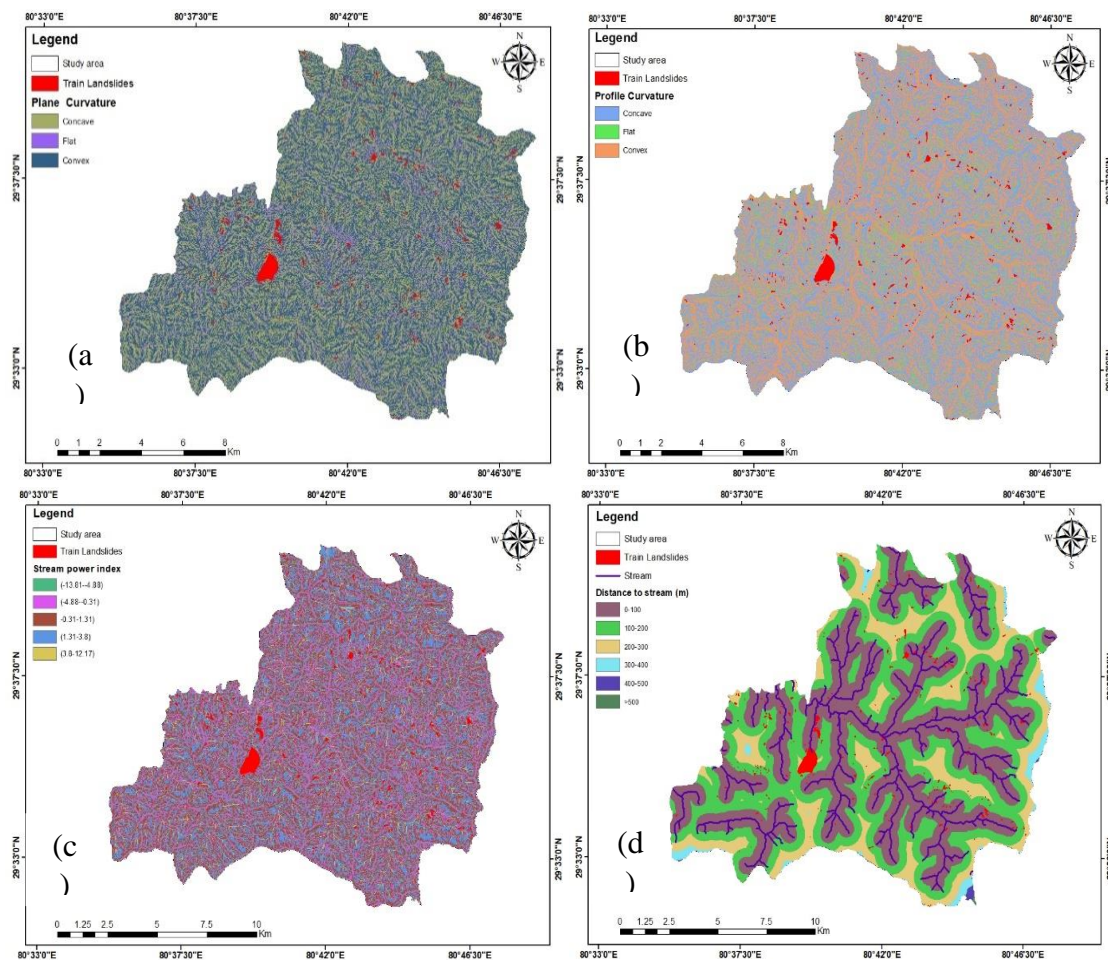

Figure 4. a) Plane curvature b) Profile curvature c) Stream power index d) Distance to stream map of the study area

Distance to the road

Research based on practical observations has indicated that poorly planned road construction, often without taking geological and geotechnical factors into account, has played a role in causing shallow landslides, as documented by studies conducted by (Shahi et al., 2022). Improper construction practices on sloping terrain, such as uncontrolled road excavation, can result in loss of support and changes in topography, leading to increased strain behind the slope and the formation of cracks. To

evaluate road proximity in this study, the Euclidean distance tool was applied, using a newly digitized polyline layer of roads obtained from topographical maps and Google Earth Pro in 2021. Within the study area, the categorical values for distance from the road ranged from 0 to 1000 meters. The values were buffered at various intervals, including 0-50, 50-100, 100-150, 150-200, and >200 meters, as shown in Fig. 5a.

Rainfall

Increased rainfall leads to elevated soil moisture levels on slopes, diminishing slope stability. Rainfall data quantifies the volume of water that descends onto the earth's surface within a specific timeframe and is denoted in millimeters (mm) (Fell et al., 2008). Rainfall data from the DHM of 13 years from 2011-2023AD of three stations (Chainpur west, Patan west and Pipalkot) were used to classify rainfall amounts in the study area. The higher the rainfall frequency, the higher the chances of landslides, as shown in Figure 5b.

Geology

The study of landslide susceptibility is influenced by geology, as it involves analyzing the varying susceptibility of different geological formations to active geomorphological processes (Pradhan et al., 2002). For this study, the geological map was obtained from the

department of Mines and Geology (DMG), Government of Nepal and digitized it in the ArcGis. The geological formations developed by DMG were used to correlate landslide with geology. There are six formations in the geological map of the study area namely: Lakharpata Formation, Galyang Formation, Ranimatta Formation, and Sallyani Gad formation. Ba, Syangja formation as illustrated in Fig. 5c.

Land cover

Land cover refers to the visible presence of physical and biological elements on the surface of the Earth. Land cover changes can impact on an area's susceptibility to landslides, either increasing or decreasing it. Geological structure, lithology, and land cover can undergo seasonal or rapid changes due to natural processes and human activities (Reichenbach et al., 2018). To evaluate the impact of land cover on landslide occurrences, it is crucial to establish the relationship between different land cover types and landslides. This correlation needs to be defined because land cover can undergo rapid changes within a short period. By studying how land cover influences landslides, researchers can assess the effects of land cover dynamics on landslide occurrences and better understand the role of land cover in landslide susceptibility (Pisano et al., 2017). The land use and land cover map are shown in Fig. 5d.
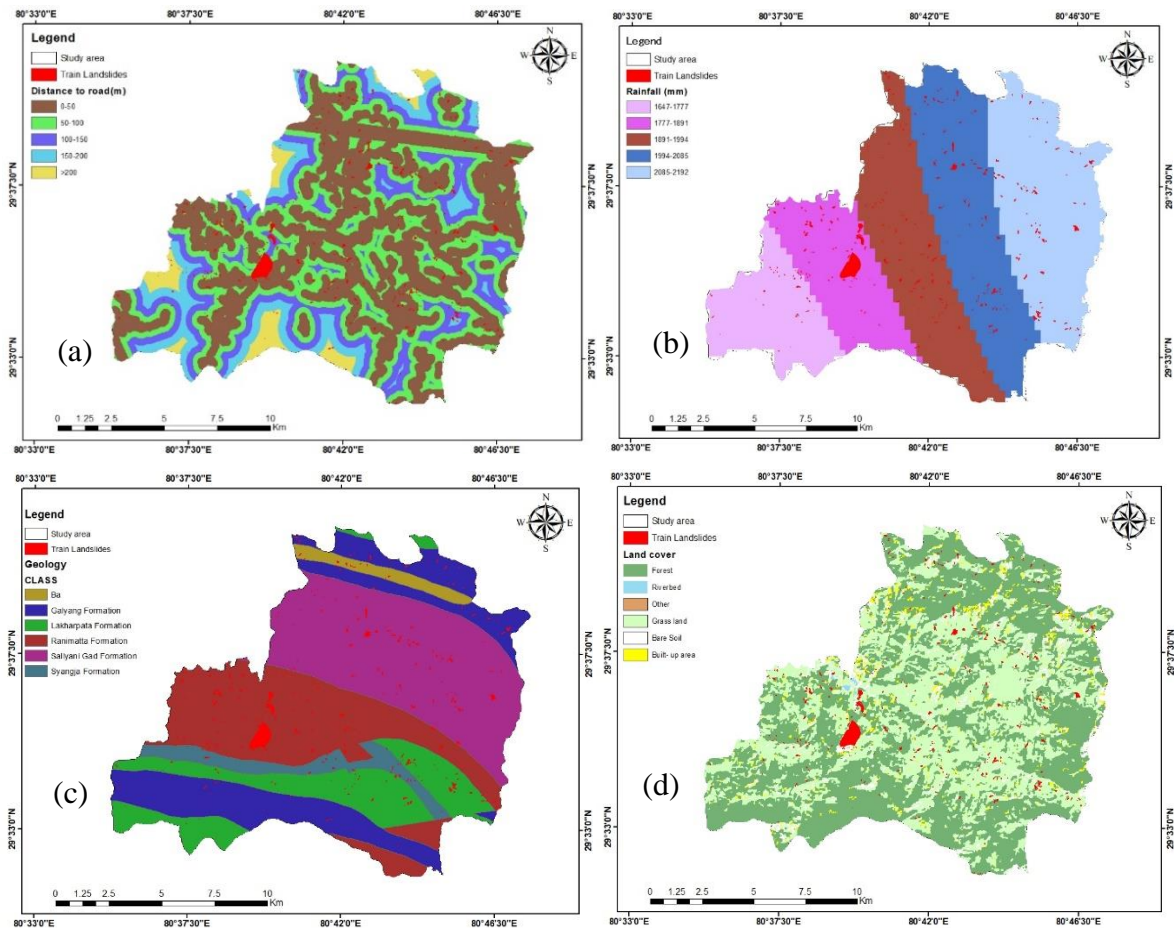

Figure 5. a) Distance to road b) Rainfall c) Geology d) Land use map of the study area

TU-CDES

Landslide inventory mapping

The inventory map of the study area was created by digitizing satellite images from Google Earth and Landsat captured between 2006 and 2021(Fig. 6). The landslides were divided into two categories: Training landslides and testing landslides. The landslides were marked as polygons and imported into ArcGIS software for further analysis. To conduct a thorough examination, the polygon-shaped landslide data was converted into raster format and then projected onto the WGS 1984 UTM zone 44N geographical coordinate system. The mapping procedure was executed with a scale of 1:25,000, and to ensure data accuracy, field surveys were conducted on-site for validation. In the inventory, 70% of the pre-existing landslides were chosen for training, while the remaining 30% consisted of current landslides reserved for testing and evaluation. Each factor map was reclassified, and the pixel area for each class in the factor map was manually recorded in ArcMap. Using cross-tabulation in ArcMap, the landslide pixel areas were extracted from the factor maps and the landslide inventory maps. To analyze the data, the FR and the WoE were applied based on the values of the class pixel area in the factor maps and the landslide pixel class area. This allowed for a comprehensive analysis of the relationship between the factor maps and the occurrence of landslides.
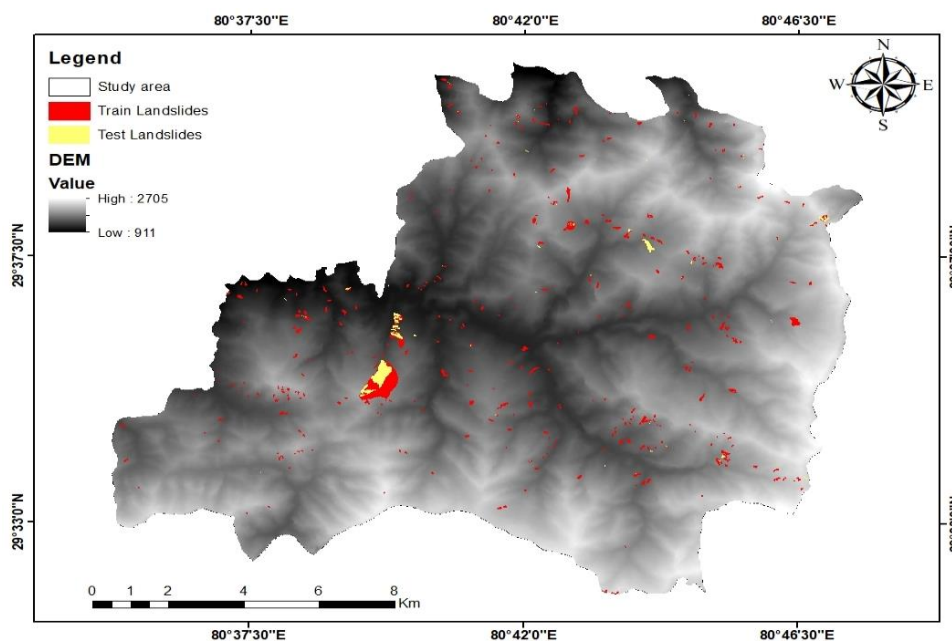

Figure 6. Landslide inventory map of the study area

Landslide susceptibility mapping
Frequency ratio model

To assess the significance of each factor in relation to landslide susceptibility, the landslide estimation group was overlaid with individual thematic data layers. Then, the FR for each class of these factors was determined through a three-step process. Initially, the calculation involved determining the ratio of the area where landslides occurred to the area where they did not occur within each class of the factor. Subsequently, the ratio of each factor's class area to the total area of that factor was computed. The formula for calculating the FR for a specific class of factors influencing landslides is detailed in Equation as outlined by Lee and Pradhan (2010) and Bhandari et al. (2024) .

$$FR = \frac{A/B}{C/D}$$

In this context, 'A' represents the count of pixels with landslides for each factor, 'B' is the total number of landslides in the study area, 'C' is the count of pixels within the class area of the factor, 'D' is the total number of pixels in the study area, and 'FR' stands for the frequency ratio of a class for the factor. The calculated ratio values using the FR were designated as weights for the classes within each factor map. These weighted factor thematic maps were then superimposed and mathematically combined using a raster calculator, following Equation as described by (Lee & Pradhan, 2010).

$$LSI = \sum Fr$$

In this equation, 'FR' represents the frequency ratio corresponding to each type or range of factors. A higher LSI pixel value indicates a greater susceptibility to landslides, while a lower pixel value suggests a lower susceptibility. Various techniques can be used to categorize landslide susceptibility indexes, including methods like equal intervals, natural breaks, and standard deviations, as outlined by (Ayalew & Yamagishi, 2005). This method divides the landslide susceptibility indexes into four distinct classes: 1) Low, 2) Moderate, 3) High, and 4) Very High.

Weight of evidence model

To assess how each factor contributes to landslide susceptibility, the landslide estimation group was

overlaid with thematic data layers individually, and the weight of evidence for each class of factors was determined through a two-step process. Initially, calculations were made for W+ and W- values based on the occurrence and non-occurrence of landslides within each class of the factor. Subsequently, an analysis of Wc was conducted. The WoE model equation conducted by Bonham-Carter (1989) and Bonham-Carter (1994) is given below in the equations.

$$W^+ = \text{Ln} \; \frac{P(\frac{B}{D})}{P(\frac{B}{\overline{D}})}$$

$$W^- = \text{Ln} \; \frac{P(\frac{\overline{B}}{D})}{P(\frac{\overline{B}}{\overline{D}})}$$

In the provided equation, 'P' stands for probability, whereas in this context, the natural logarithm is involved. 'B' and 'B $^\top$' represent the presence and absence of potential landslide evidence factors, respectively. Similarly, 'D' and 'D $^\top$' denote the presence and absence of landslides, respectively. To compute the significance of each causal factor contributing to landslide occurrences, as described by Van Westen et al. (2003) have been employed.

$$W^+ = \ln\{(\frac{[Npix1]}{[Npix1]+[Npix2]})/(\frac{[Npix3]}{[Npix3]+[Npix4]})\}$$

$$W^- = \ln\{(\frac{[Npix3]}{[Npix1]+[Npix2]})/(\frac{[Npix4]}{[Npix3]+[Npix4]})\}$$

Npix1 is the number of pixels expressing the existence of both landslide contributing factors and landslide; Npix2 represents the presence of landslide and absence of landslide and absence of landslide contributing factor. While Npix3 means the presence of landslide contributing factors and the absence of landslide. Similarly, Npix4 represents the absence of both landslide and landslide contributing factors. The final weight expressed with W^c was calculated using the following Equation.

$$W^c = (W^+) - (W^-)$$

Where W^c is the difference between W$^+$ and W$^-$. This elucidates the spatial relationship of all landslides contributing factors and landslides. This method classified landslide susceptibility indexes into four susceptible classes 1) Low, 2) Moderate, 3) High, and 4) Very High.

Model validation

In research, after data analysis, map validation is necessary to check the data's accuracy. In modern times there are different tools developed which help easily determine how much our analyzed data is valid or accurate.

The final step in landslide susceptibility analysis entails verifying the reliability of the projected results. There are several methods available for validating the LSI map, including approaches like ROC analysis as described by Mathew et al. (2007) and the AUC method employing

success rate curve or prediction rate curve. In the present study, the landslide susceptibility maps were verified utilizing the success rate and prediction rate curves (Xu et al., 2013) to validate the prediction results. The success rate curve was obtained from the ArcMap when Arc- SDM software was installed on the desktop and added to the Arc toolbox. Arc SDM software was opened through the ROC tool in the Arc toolbox. From the ROC tool, prediction and success curve was generated by manually using training and testing points in input and LSP in the output section for both models. The LDR method was also applied for data validation. Landslide density was determined by comparing the area of specific susceptibility classes to the area of landslides within those classes. It was noticed that the various susceptibility zones identified through both methods had nearly equal areas.

Results and Discussion
Landslide Inventory Map

Altogether 515 landslides were traced out in the inventory map. Out of 515 landslides, 365 (making up 70%) were allocated for training purposes, representing older landslides. The remaining 150 (constituting 30%) were reserved for validation and represented currently active landslides. Within the testing landslides, 13 were found in the Ruinigad catchment area, 7 in the Baggad catchment area, and 10 in the Loligad catchment area. Furthermore, 90 landslides were found downstream of Tribeni. The Danpur landslide, located within the Tribeni watershed, was identified as the largest landslide.

Additionally, 15 landslides were observed outside the Tribeni catchment. The study area encompasses a total area of 198.5 km², and the landslides are unevenly distributed throughout this region. Upon comparing the training and testing inventory maps, it was evident that most of the landslides overlay each other, indicating that active landslides occur on top of pre-existing landslides, particularly near the streamside. The inventory map shows a large landslide in Dandpur, Chimada, and Kimet Budada. The temporal inventory map of Dandapur shows that the area of landslide is frequently increasing on the top side over time.

Landslide Susceptibility

Landslide susceptibility maps plot the potential for landslides to occur in a region as a function of the environmental conditions of the area. These susceptibility maps describe the size and spatial distribution of landslide occurrences in the region and can influence regional hazard mitigation and relief plans (Mezughi et al., 2011; Mondal & Mandal, 2019). The success rate is a calculation of the success of a model that shows how well the model matches the prior events (Chung & Fabbri, 2003). The landslide susceptibility mas was created using the FR and WoE models. In both models, factor maps were computed by reclassifying each individual factor map and superimposing them with the training landslide data. Compared to the southern part, the northern and eastern parts of the study area

exhibit a high to extremely high class of susceptibility. The proportions of medium and high susceptibility classes exceed those of low and very high susceptibility classes. Overall, 33.49% of the region is classified as high susceptibility, while 30.88% is classified as moderate susceptibility. Only 16.91% of the area falls into the very

high susceptibility class. 35.05% of the landslide's total area falls into the intermediate susceptibility class. Figure 7 illustrates the landslide susceptibility map generated utilizing the FR model. Furthermore, Fig. 8 illustrates the percentage distribution of susceptibility classes and landslide occurrences derived from the FR model.
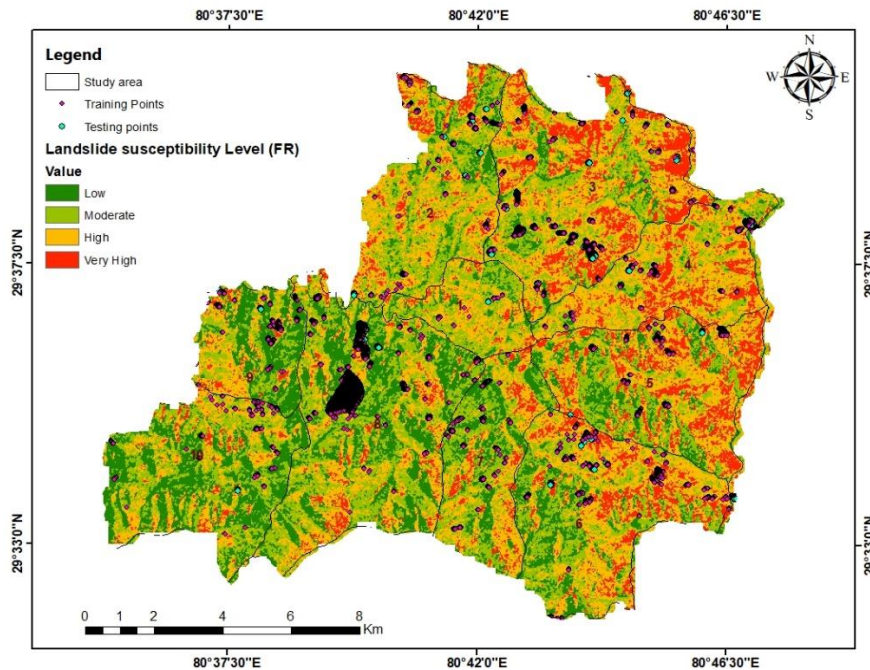

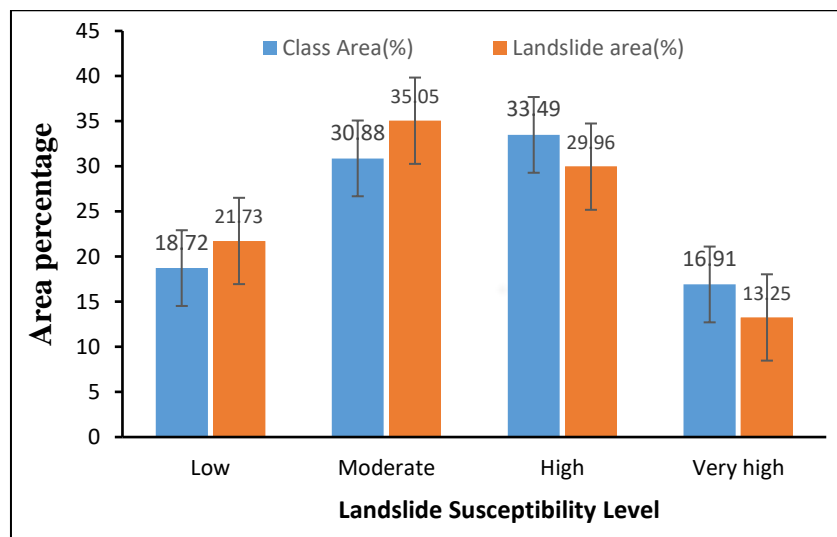**Figure 7.** Landslide susceptibility map by using frequency ratio model

Figure 8. Percentage distribution of the susceptibility classes and landslide occurrence by using FR model

The landslide susceptibility map by using WoE model is shown in Fig. 9 **a**nd percentage distribution of the susceptibility classes and landslide occurrence by using WoE Model is given in Fig. 10. The result is more or less similar to the FR model. The northern and eastern parts of the study area are found to have high to very high susceptibility in comparison to the southern and south-

western parts. The percentages of medium and high susceptibility classes are greater than low and very high. The high susceptibility class occupies 33.82% of the area, while the moderate susceptibility class occupies 30.52%. Very high-susceptibility classes occupy only 17.06% of the area. 35.1% of the total landslide area falls into the moderate susceptibility class.
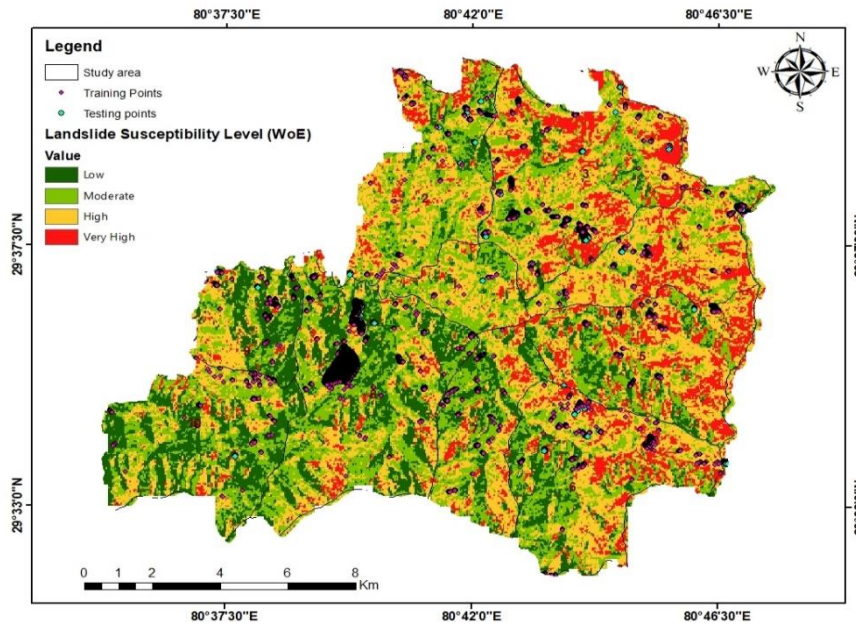
TU-CDES

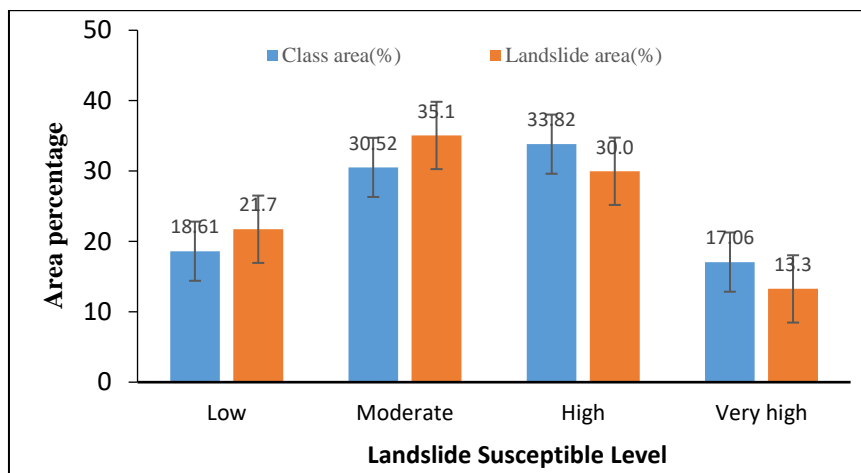**Figure 9.** Landslide susceptibility by weight of evidence model

Figure 10. Percentage distribution of the susceptibility classes and landslide occurrence by using WoE Model

Landslides density percentage analysis

Density is typically computed by determining the proportion of the area belonging to a specific susceptibility category relative to the area impacted by landslides within that category. Interestingly, the distinct susceptible zones categorized under both approaches exhibit nearly identical areas. Consequently, with respect to landslide occurrence areas, both methodologies have displayed outstanding outcomes, significantly enhancing the credibility and verification of both models in the context of identifying regions susceptible to landslides.

It has been observed that the landslide densities derived from both methodologies exhibit a gradual increase from the lowest susceptibility class, 'Very Low,' to the highest, 'Very High' (Figs. 11a, 11b). This observed trend further affirms the accuracy and effectiveness of the susceptibility classification scheme employed in this Landslide study (Neupane et al., 2023).

AUC validation

The success and prediction rate of the two models are shown in Fig. 12 (a, b, c, and d). Validation datasets collected during fieldwork were used to verify the two landslide susceptibility models' predictions in this study. Figure 12 shows the performance of the model using the area under the curve (AUC). The results show that both models are capable of accurately predicting susceptibility. Because of this, both models demonstrated similar prediction and success rate, and it is highly acceptable. The prediction rate of both models is 0.703. Similarly, the success rate of both models is genuine and acceptable: FR (0.777) and WoE (0.775). In terms of mapping landslide susceptibility in the research area, similar result obtained from both models. Based on the validation result, any of the models can be used for landslides susceptibility in the similar region.
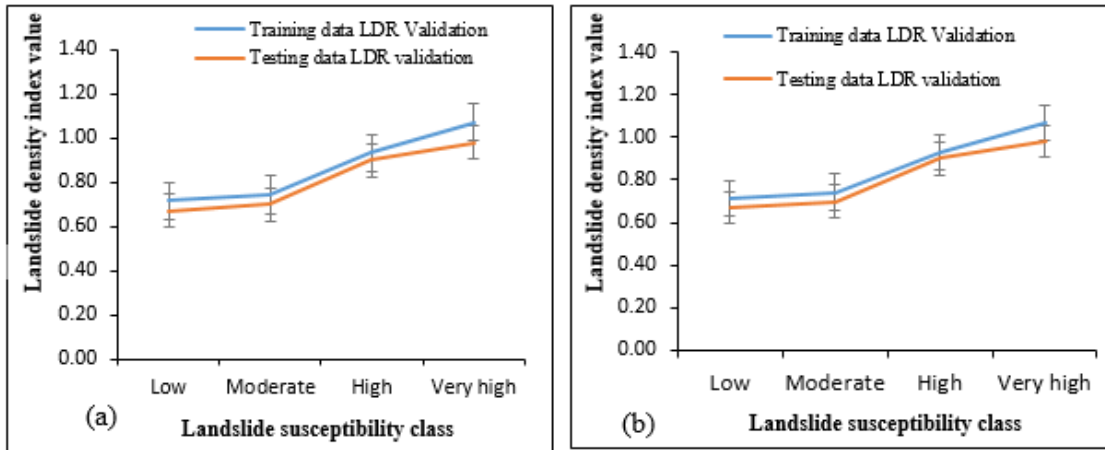
TU-CDES

Figure 11. LDR validation of a) FR method b) WoE method of the study area
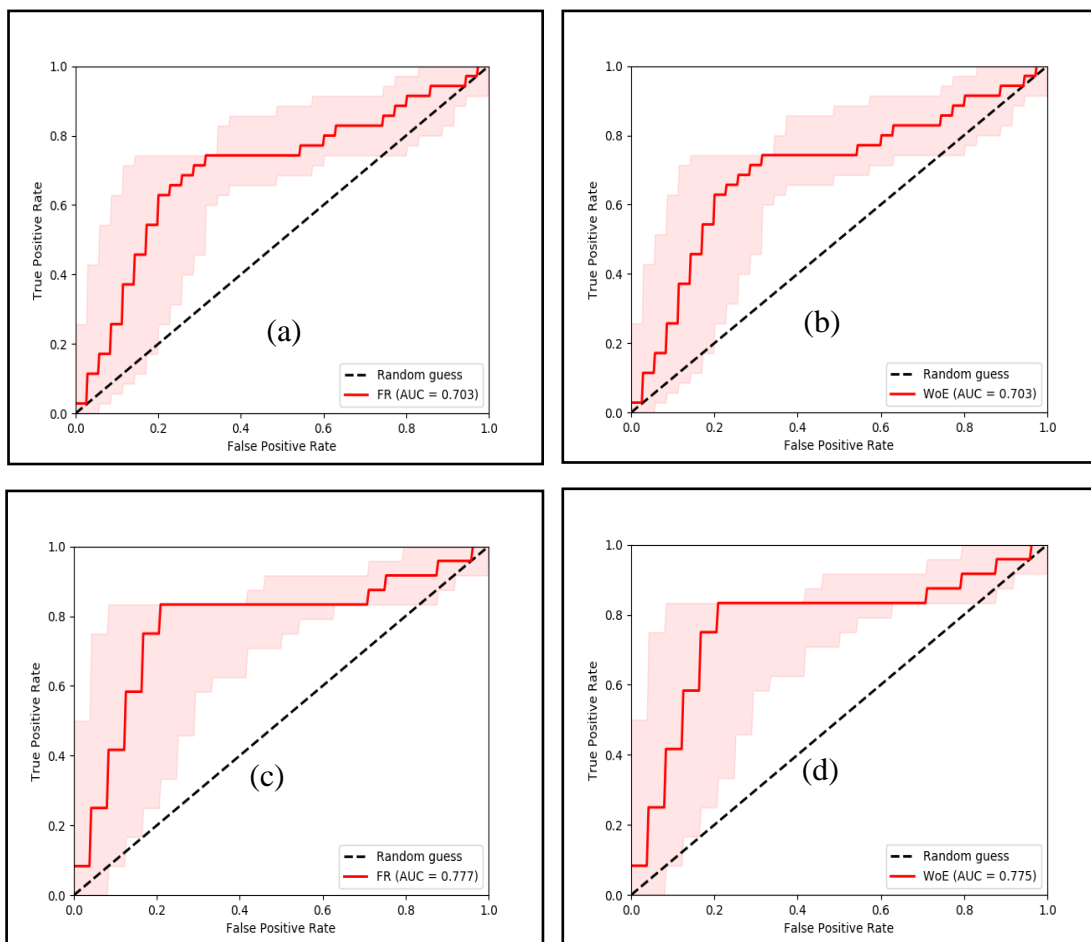

Figure 12. Area Under Curve shows a) prediction rate curve of landslide susceptibility by FR model b) WoE model c) success rate curve of landslide susceptibility by FR model d) success rate curve of landslide susceptibility by WoE model

Regmi et al. (2013) employed Fr, WoE, and SI models to evaluate landslide susceptibility mapping in the Central Nepal Himalaya region. In their result, the FR model exhibited the highest performance, achieving a success rate of 76.8% and a predicted accuracy of 75.4%, according to the statistics. The study conducted by Pham et al., (2015) shows that the FR model exhibited a 75% success accuracy and a 70% prediction accuracy. Regmi et al., (2014) performed a study that attained a success accuracy of 83.31% and a prediction accuracy of 78.58% by using FR model in the Bhalubang–Shivapur Area of Nepal. The study conducted by Bhandari et al. (2024)

obtained higher prediction and success rate by FR model in the Siwalik zone of Nepal. Previous research conducted in Nepal indicated that individual FR and WoE yielded a superior prediction rate. In the previously referenced studies, the FR model demonstrated superior performance in the Nepal Himalaya for landslide susceptibility (Bhandari et al., 2024). Thapa and Bhandari (2019) obtained more than 75% success and prediction rate by using FR model in the Siwalik section of Nepal. Nevertheless, the WoE model exhibited exceptional performance in terms of both the rate of success and the rate of prediction in the Lesser Himalaya region of Nepal.

In this study, the training data for the two susceptibility models showed a fair level of goodness of fit. There is no significant difference in the success and prediction rate in both models, however, FR model shows a slightly better level of prediction. This is apparent from the area under the Curve (AUC) readings of the Receiver Operating Characteristic (ROC), which reaches a value of 0.777. The study found that the FR model achieved a success rate of 77.7%. FR achieved an area under the curve (AUC) value of 0.777, whereas the WoE models had AUC values of 0.775. The correlation between the training data and validation data on landslide occurrences indicates a satisfactory level of concurrence. The majority of pixels that encountered landslides were categorized as having a significant or elevated susceptibility in both models.

Conclusions
In this study, landslide susceptibility maps were created by using bivariate models that utilized both the frequency ratio and weight of evidence methods. Initially, 70% of the data was randomly selected for training the model, while the remaining 30% was used for validation purposes. Twelve distinct factors were and these were factor maps were integrated into the modeling process using ArcGIS. Subsequently, the prepared landslide susceptibility maps were categorized into four classes, ranging from "Low" to "Very High," by using the natural break method. In both modeling methods, the density of landslides slightly increases as we move from the Low susceptibility class to the Very High susceptibility class. Notably, the moderate and high susceptibility classes cover a significantly larger area compared to the low and very high classes. The success rate curves for both models exhibited an identical value of 77.77%. Similarly, the prediction rate curves for FR and WoE also yielded equivalent results, both at 70.2%. With both methods achieving an accuracy level exceeding 70%, the findings are considered reasonable. Both of the models are suitable for the development of susceptibility maps in the similar terrains in the Sudurpaschim province. The landslide susceptibility map generated from this study is valuable for the study area in formulating a disaster risk management plan and procedural actions. These findings may serve as a reference for future studies in similar terrains in

Sudurpaschim province and other regions of the country.

Author contributions: BPB: Created the concept, methods, and editing and finalized the manuscript; PBA collected the data and prepared the manuscript.

Conflicts of interest: The authors declare no competing interests.

Data Availability Statement: The authors confirm that the data supporting the findings of this study are available within the article.

References
Aleotti, P., & Chowdhury, R. (1999). Landslide hazard assessment: Summary review and new perspectives. *Bulletin of Engineering Geology and the Environment*, 58(1), 21–44. https://doi.org/10.1007/s100640050066.

Armaş, I. (2012). Weights of evidence method for landslide susceptibility mapping. Prahova Subcarpathians, Romania. *Natural Hazards*, 60(3), 937–950. https://doi.org/10.1007/s11069-011-9879-4.

Ayalew, L., & Yamagishi, H. (2005). The application of GIS-based logistic regression for landslide susceptibility mapping in the Kakuda-Yahiko Mountains, Central Japan. *Geomorphology*, 65(1–2), 15–31.

Beven, K.J., & Kirkby, M.J. (1979). A physically based, variable contributing area model of basin hydrology/Un modèle à base physique de zone d'appel variable de l'hydrologie du bassin versant. *Hydrological Sciences Journal*, 24(1), 43–69.

Bhandari, B.P., & Dhakal, S. (2021). Decadal Evolution of Landslides in the Siwalik Zone: a Case Study of Babai Watershed, Nepal. *Journal of Institute of Science and Technology*, *26*(1), 57–62. https://doi.org/10.3126/jist.v26i1.37864.

Bhandari, B.P., Dhakal, S., & Tsou, C.-Y. (2024). Assessing the Prediction Accuracy of Frequency Ratio, Weight of Evidence, Shannon Entropy, and Information Value Methods for Landslide Susceptibility in the Siwalik Hills of Nepal. *Sustainability*, 16(5), 2092.

Bonham-Carter, G.F. (1989). Weights of evidence modelling: A new approach to mapping mineral potential. *Statistical Applications in the Earth Sciences*, 13, 171–183.

Bonham-Carter, G.F. (1994). Geographic information systems for geoscientists-modeling with GIS. *Computer Methods in the Geoscientists*, 13, 398.

Burt, T., & Butcher, D. (1986). Stimulation from simulation? A teaching model of hillslope hydrology

for use on microcomputers. *Journal of Geography in Higher Education*, 10(1), 23–39.

Chung, C.-J.F., & Fabbri, A.G. (2003). Validation of spatial prediction models for landslide hazard mapping. *Natural Hazards*, 30, 451–472.

Collins, B.D., Kayen, R., & Tanaka, Y. (2012). Spatial distribution of landslides triggered from the 2007 Niigata Chuetsu–Oki Japan Earthquake. *Engineering Geology*, 127, 14–26.

Cruden, D.M., & Varnes, D.J. (1996). *Landslides: Investigation and Mitigation*. Transportation Research Board Special Report, 247.

Dai, F.C., Xu, C., Yao, X., Xu, L., Tu, X.B., & Gong, Q.M. (2011). Spatial Distribution of Landslides Triggered by the 2008 Ms 8.0 Wenchuan Earthquake, China. *Journal of Asian Earth Sciences, 40,* 883-895. https://doi.org/10.1016/j.jseaes.2010.04.010.

Ercanoglu, M., Kasmer, O., & Temiz, N. (2008). Adaptation and comparison of expert opinion to analytical hierarchy process for landslide susceptibility mapping. *Bulletin of Engineering Geology and the Environment*, 67(4), 565–578. https://doi.org/10.1007/s10064-008-0170-1.

Fell, R., Corominas, J., Bonnard, C., Cascini, L., Leroi, E., & Savage, W.Z. (2008). Guidelines for landslide susceptibility, hazard and risk zoning for land use planning. *Engineering Geology*, 102(3–4), 85–98.

Getachew, N., & Meten, M. (2021). Weights of evidence modeling for landslide susceptibility mapping of Kabi-Gebro locality, Gundomeskel area, Central Ethiopia. *Geoenvironmental Disasters*, 8(1), 6. https://doi.org/10.1186/s40677-021-00177-z.

Guzzetti, F., Mondini, A.C., Cardinali, M., Fiorucci, F., Santangelo, M., & Chang, K.T. (2012). Landslide inventory maps: New tools for an old problem. *Earth Science Reviews*, 112(1-2), 42-66.

Hamza, T., & Raghuvanshi, T.K. (2017). GIS based landslide hazard evaluation and zonation–A case from Jeldu District, Central Ethiopia. *Journal of King Saud University-Science*, 29(2), 151–165.

Hung, L.Q., Van, N.T.H., Son, P.V., Ninh, N.H., Tam, N., & Huyen, N.T. (2017). Landslide Inventory Mapping in the Fourteen Northern Provinces of Vietnam: Achievements and Difficulties. In K. Sassa, M. Mikoš, & Y. Yin (Eds.), *Advancing Culture of Living with Landslides* (pp. 501–510). Springer International Publishing. https://doi.org/10.1007/978-3-319-59469-9_44.

Jana, S.K., Sekac, T., & Pal, D.K. (2019). Geo-spatial approach with frequency ratio method in landslide susceptibility mapping in the Busu River catchment, Papua New Guinea. *Spatial Information Research*, 27(1), 49–62. https://doi.org/10.1007/s41324-018-0215-x.

Karimi, S.E., Ownegh, M., Sadaldin, A., & Mashayekhan, A. (2011). *Probabilistic Landslide Risk Analysis and Mapping (Case Study: Chehel-Chai Watershed, Golestan Province, Iran)*.

Kavzoglu, T., Sahin, E.K., & Colkesen, I. (2014). Landslide susceptibility mapping using GIS-based multi-criteria decision analysis, support vector

machines, and logistic regression. *Landslides*, 11, 425–439.

Kayastha, P., Dhital, M.R., & De Smedt, F. (2013). Application of the analytical hierarchy process (AHP) for landslide susceptibility mapping: A case study from the Tinau watershed, west Nepal. *Computers & Geosciences*, 52, 398–408.

Khan, H., Shafique, M., Khan, M.A., Bacha, M.A., Shah, S.U., & Calligaris, C. (2019). Landslide susceptibility assessment using Frequency Ratio, a case study of northern Pakistan. *The Egyptian Journal of Remote Sensing and Space Science*, 22(1), 11–24.

Lee, S., & Min, K. (2001). Statistical analysis of landslide susceptibility at Yongin, Korea. *Environmental Geology*, 40, 1095-1113.

Lee, S., & Pradhan, B. (2010). Landslide hazard mapping at Selangor, Malaysia using frequency ratio and logistic regression models. *Landslides*, 4(1), 33–41.

Lee, S., & Sambath, T. (2006). Landslide susceptibility mapping in the Damrei Romel area, Cambodia using frequency ratio and logistic regression models. *Environmental Geology*, 50(6), 847–855. https://doi.org/10.1007/s00254-006-0256-7.

Manchado, M.T., Allen, A.S., Ballesteros-Canovas, J.A., Dhakal, A., Dhital, M.R., Stoffel, M. (2021). Three decades of landslide activity in Western Nepal: New insights into trends and climate drivers. *Landslides*, 18, 2001–2015.

Mathew, J., Jha, V., & Rawat, G. (2007). Application of binary logistic regression analysis and its validation for landslide susceptibility mapping in part of Garhwal Himalaya, India. *International Journal of Remote Sensing*, 28(10), 2257–2275.

Mezughi, T.H., Akhir, J.M., Rafek, A.G., & Abdullah, I. (2011). Landslide susceptibility assessment using frequency ratio model applied to an area along the EW highway (Gerik-Jeli). *American Journal of Environmental Sciences*, 7(1), 43.

Mondal, S., & Mandal, S. (2019). Landslide susceptibility mapping of Darjeeling Himalaya, India using index of entropy (IOE) model. *Applied Geomatics*, 11(2), 129–146. https://doi.org/10.1007/s12518-018-0248-9

Moore, I.D., Grayson, R., & Ladson, A. (1991). Digital terrain modelling: A review of hydrological, geomorphological, and biological applications. *Hydrological Processes*, 5(1), 3–30.

Petley, D. (2012). Global patterns of loss of life from landslides. *Geology*, 40(10), 927–930.

Pisano, L., Zumpano, V., Malek, Ž., Rosskopf, C.M., & Parise, M. (2017). Variations in the susceptibility to landslides, as a consequence of land cover changes: A look to the past, and another towards the future. *Science of The Total Environment*, 601, 1147–1159.

Pokhrel, K., & Bhandari, B.P. (2019). Identification of potential landslide susceptible area in the lesser Himalayan Terrain of Nepal. *Journal of Geoscience and Environment Protection*, 7(11), 24–38.

Pourghasemi, H.R., Teimoori Yansari, Z., Panagos, P., & Pradhan, B. (2018). Analysis and evaluation of landslide susceptibility: A review on articles published during 2005–2016 (periods of 2005–2012

and 2013–2016). *Arabian Journal of Geosciences*, 11(9), 193. https://doi.org/10.1007/s12517-018-3531-5.

Pradhan, B. (2010). Landslide susceptibility mapping of a catchment area using frequency ratio, fuzzy logic and multivariate logistic regression approaches. *Journal of the Indian Society of Remote Sensing*, 38(2), 301–320. https://doi.org/10.1007/s12524-010-0020-z.

Pradhan, U., Shrestha, R., KC, S., & Sharma, S. (2002). *Geological map of petroleum exploration block—7, Malangawa, Central Nepal (Scale: 1: 250,000)*. Petroleum Exploration Promotion Project, Department of Mines and Geology, Kathmandu.

Rasyid, A.R., Bhandary, N.P., & Yatabe, R. (2016). Performance of frequency ratio and logistic regression model in creating GIS based landslides susceptibility map at Lompobattang Mountain, Indonesia. *Geoenvironmental Disasters*, 3(1), 19. https://doi.org/10.1186/s40677-016-0053-x.

Regmi, A.D., Devkota, K.C., Yoshida, K., Pradhan, B., Pourghasemi, H.R., Kumamoto, T., Akgun, A. (2013). Application of frequency ratio, statistical index, and Weights-of-evidence models and their comparison in landslide susceptibility mapping in Central Nepal Himalaya. *Arabian Journal of Geosciences*, 7, 725–742.

Regmi, A.D., Devkota, K.C., Yoshida, K., Pradhan, B., Pourghasemi, H. R., Kumamoto, T., & Akgun, A. (2014). Application of frequency ratio, statistical index, and weights-of-evidence models and their comparison in landslide susceptibility mapping in Central Nepal Himalaya. *Arabian Journal of Geosciences*, 7, 725–742.

Reichenbach, P., Rossi, M., Malamud, B.D., Mihir, M., & Guzzetti, F. (2018). A review of statistically-based landslide susceptibility models. *Earth-Science Reviews*, 180, 60–91.

Shahi, Y. B., Kadel, S., Dangi, H., Adhikari, G., KC, D., & Paudyal, K. R. (2022). Geological Exploration, Landslide Characterization and Susceptibility Mapping at the Boundary between Two Crystalline Bodies in Jajarkot, Nepal. *Geotechnics*, 2(4), 1059–1083.

Sun, X., Chen, J., Li, Y., & Rene, N.N. (2022). Landslide Susceptibility mapping along a rapidly uplifting river valley of the Upper Jinsha River, Southeastern Tibetan Plateau, China. *Remote Sensing*, 14(7), 1730.

Thapa, D., & Bhandari, B.P. (2019). GIS-Based frequency ratio method for identification of potential landslide susceptible area in the Siwalik zone of Chatara-Barahakshetra section, Nepal. *Open Journal of Geology*, 9(12), 873.

Thapa, P. B. (2015). Occurrence of landslides in Nepal and their mitigation options. *Journal of Nepal Geological Society*, 49(1), 17–28.

Van Westen, C., Rengers, N., & Soeters, R. (2003). Use of geomorphological information in indirect landslide susceptibility assessment. *Natural Hazards*, 30, 399–419.

Xu, C., Xu, X., Dai, F., Wu, Z., He, H., Shi, F., Wu, X., & Xu, S. (2013). Application of an incomplete landslide inventory, logistic regression model and its validation for landslide susceptibility mapping related to the May 12, 2008 Wenchuan earthquake of China. *Natural Hazards*, 68, 883–900.

Zhu, A.-X., Wang, R., Qiao, J., Qin, C.-Z., Chen, Y., Liu, J., Du, F., Lin, Y., & Zhu, T. (2014). An expert knowledge-based approach to landslide susceptibility mapping using GIS and fuzzy logic. *Geomorphology*, 214, 128–138.